13. K. D. Croen, *J. Clin. Invest.* **91**, 2446 (1993); G. Karupiah *et al.*, *Science* **261**, 1445 (1993).
14. The EFs were prepared from 12- to 14-day-old embryos, cultured in Dulbecco's modified minimum essential medium with 10% fetal calf serum, and seeded at 2.5×10^5 cells per well into 24-well plates. The cells were treated with immunoaffinity-purified natural murine IFN-α (Sumitomo Pharmaceutical, Osaka, Japan) or recombinant murine IFN-γ (Genzyme, Cambridge, MA) 18 hours before and throughout infection. EMCV, VSV, and HSV were allowed to adsorb for 1.5 hours at a concentration of 10, 0.01, and 0.1 plaque-forming units per cell, respectively, and the cells were washed twice with serum-free medium and replenished with 1 ml of medium. Half of the sample was harvested immediately to determine the titer of adsorbed viruses, and the remaining half was harvested 24 hours later to determine the titer of replicated viruses. After harvest, the cells were lysed by three cycles of freeze-thawing and sonication to recover EMCV and HSV or lysed by two cycles of freeze-thawing to recover VSV. Serially diluted virus samples were added to L cell or Vero cell monolayers to determine the yield of infectious virus in terms of plaque-forming units. After 2 to 3 days, viral plaques were counted after staining with 0.02% (w/v) neutral red. The IFNs present in the medium did not affect the efficiency of plaque formation on the L cell monolayer when virus samples were diluted more than 100 times.
15. K. Nakayama, T. Kimura, T. Taniguchi, unpublished observations.
16. To obtain mice lacking both *IRF-1* and *IRF-2* genes, we first generated IRF-$1^{+/-}$ IRF-$2^{+/-}$ mice by interbreeding IRF-$1^{-/-}$ mice and IRF-$2^{-/-}$ mice. After intercrossing these heterozygous mice, we obtained IRF-$1^{-/-}$ IRF-$2^{-/-}$ mice. The genotype of the mice was determined by polymerase chain reaction analysis, and the lack of IRF-1 and IRF-2 activities in the EFs was confirmed by gel mobility-shift assay (*10*).
17. J. Penninger, unpublished observations.
18. B. R. Murphy and L. A. Glasgow, *J. Exp. Med.* **127**, 1035 (1968); L. A. Glasgow, *J. Gen. Physiol.* **56** (suppl.), 212 (1970).
19. B. A. Hassel, A. Zhou, C. Sotomayor, A. Maran, R. H. Silverman, *EMBO J.* **12**, 3297 (1993).
20. Y.-S. E. Cheng, C. E. Patterson, P. Staeheli, *Mol. Cell. Biol.* **11**, 4717 (1991); T. A. Wynn, C. M. Nicolet, D. M. Paulnock, *J. Immunol.* **147**, 4384 (1991); S. L. Anderson, J. Lou, L. Xing, R. Witkus, B. Y. Rubin, *J. Interferon Res.* **12**, S86 (1992); P. Constantoulakis *et al.*, *Science* **259**, 1314 (1993).
21. D. G. Fischer, N. Tal, D. Novick, S. Barak, M. Rubinstein, *Science* **262**, 250 (1993).
22. The *GBP* genes have been known as *GBP-1 (mag-1)* and *minor GBP* (including *mag-2*), and our probe can detect mRNA from both *GBP-1* and 2.5-kb *minor GBP* (*20*). Because these EFs do not express the *GBP-1* gene (*15*), the mRNA signal indicates expression of the 2.5-kb *minor GBP* gene.
23. A. M. A. Imam, A. M. Ackrill, T. C. Dale, I. M. Kerr, G. R. Stark, *Nucleic Acids Res.* **18**, 6573 (1990); J. Parrington *et al.*, *Eur. J. Biochem.* **214**, 617 (1993).
24. J. John *et al.*, *Mol. Cell. Biol.* **11**, 4189 (1991); R. McKendry *et al.*, *Proc. Natl. Acad. Sci. U.S.A.* **88**, 11455 (1991); K. Shuai, C. Schindler, V. R. Prezioso, J. E. Darnell Jr., *Science* **258**, 1808 (1992); G. R. Stark, and I. M. Kerr, *J. Interferon Res.* **12**, 147 (1992); M. Müller *et al.*, *EMBO J.* **12**, 4221 (1993); S. Pellegrini and C. Schindler, *Trends Biochem. Sci.* **18**, 338 (1993); K. Shuai, G. R. Stark, I. M. Kerr, J. E. Darnell Jr., *Science* **261**, 1744 (1993).
25. H. Yamamoto, T. Fujita, T. Taniguchi, unpublished results.
26. H. Harada *et al.*, *Science* **259**, 971 (1993); C. L. Willman *et al.*, *ibid.*, p. 968; N. Tanaka *et al.*, *Cell*, in press.
27. RNA blotting analysis was carried out as described (*7*). Probes for *PKR, 1-8, 2-5A synthetase*, and *β-actin* were prepared as described (*10*). The probe for *iNOS* was cloned from murine macrophage RNA. Probes for *GBP* and *9-27* were a 700-bp Bam HI–Eco RI fragment of pSP65-mGBP-1 and a 300-bp Spe I–Sty I fragment of Ldk927, respectively (*20*). The specific activity of each probe was approximately 5×10^8 cpm/μg.
28. We thank S. Nagata for EMCV; K. Matsuoka and T. Yamaoka for natural murine IFN-α, L cells, and VSV; Y. Shimomura for Vero cells and HSV (Shintani strain); T. Decker for murine *GBP-1* cDNA; G. Pavlakis for human *9-27* cDNA; and E. Barsoumian, M. Lamphier, Y. Higashi and R. Yamaguchi for advice. Animal care was in accordance with institutional guidelines of Osaka University. Supported by grants from Special Project Research Cancer Bioscience of Japan, Takeda Science Foundation, the Medical Research Council of Canada, the National Science and Engineering Research Council of Canada, and the Human Frontier Science Program and by grant R35CA49731 from the National Cancer Institute.

16 February 1994; accepted 4 May 1994

Expanding the Scope of RNA Catalysis

James R. Prudent, Tetsuo Uno, Peter G. Schultz*

The basic notions of transition state theory have been exploited in the past to generate highly selective catalysts from the vast library of antibody molecules in the immune system. These same ideas were used to isolate an RNA molecule, from a large library of RNAs, that catalyzes the isomerization of a bridged biphenyl. The RNA-catalyzed reaction displays Michaelis-Menten kinetics with a catalytic rate constant (k_{cat}) of 2.8×10^{-5} per minute and a Michaelis constant (K_m) of 542 μM; the reaction is competitively inhibited by the planar transition state analog with an inhibition constant (K_i) value of ~7 μM. This approach may provide a general strategy for expanding the scope of RNA catalysis beyond those reactions in which the substrates are nucleic acids or nucleic acid derivatives.

Many of the complex problems associated with biomolecular recognition and catalysis have been solved in nature by the generation and screening of large populations of molecules. This can occur on an evolutionary time scale or over the course of a few weeks during the immune response. One of the first examples in which the chemical potential of these processes was exploited was the use of transition state theory to select from the tremendous diversity of the immune system antibodies with catalytic activities (*1*). More recently, a number of methods have been developed for generating and screening large libraries of biological or synthetic molecules in vitro for their abilities to bind selectively or transform chemically a target molecule (*2*).

One application of these methods has been the search for RNAs with previously unidentified activities (*3*). RNA has been shown to efficiently catalyze reactions involving phosphoryl group transfers (*4*), but if one is to believe in a prebiotic world in which RNA was the primitive macromolecular catalyst, other basic chemical reactions should be amenable to RNA catalysis (*5*). Moreover, many of these reactions will require substrate binding by interactions other than Watson-Crick base pairing. In an effort to begin an exploration of the catalytic repertoire of RNA, we have screened a large library of RNA molecules for the ability to bind the near-planar transition state analog **3** and catalyze the isomerization of biphenyl **1** to its diastereomer **2** (Fig. 1).

The isomerization of substituted biphenyls is a well-characterized reaction involving rotation around a C–C sigma bond (Fig. 1) (*6*). Nonbonded interactions and angle strain in the planar transition state lead to a significant barrier to isomerization. As a result, isomeric substituted biphenyls can be isolated and interconvert quite slowly at room temperature. On the basis of Pauling's notion of enzymatic catalysis, in which maximum binding occurs to the transition state (TS‡) rather than to either substrates or products (*7*), an RNA that preferentially binds an analog of the planar transition state **4** should have the potential to catalyze the isomerization of substrate **1** to product **2**. This reaction provides one of the simplest systems in which to test this notion (*8*); it is unlikely that any other mechanisms such as general acid-base, metal ion, or electrostatic catalysis would be operative in this reaction.

The isomerization of the 10-membered ring bridged biphenyl **1** to its diastereomer **2** was chosen as a model system. The x-ray crystal structure of **2** reveals a dihedral angle between the two aryl rings of 68° (0° is coplanar). The near-planar phenanthrene derivative **3** was chosen as a mimic of the planar transition state **4** because bridged biphenyls of this sort are known to have dihedral angles of ~15° (*9*). In order to simplify substrate isolation and analysis of substrate to product ratios, we introduced

Department of Chemistry, University of California, and Lawrence Berkeley Laboratory, Berkeley, CA 94720, USA.

*To whom correspondence should be addressed.

a chiral center into the 10-membered ring bridge to generate diastereomeric substrate **1** and product **2**. Condensation of 2,2′-bis(bromomethyl)biphenyl (*10*) with the disodium salt of (*S*)-1,2-propanediol alkoxide, followed by chromatography on silica gel and recrystallization from petroleum ether afforded pure substrate **1** and product **2** (*11*). The TS‡ analog **3** was synthesized by oxidation of phenathrene with osmium tetroxide, acid-catalyzed condensation of the resulting diol with adipic aldehyde methyl ester, and subsequent saponification under basic conditions to yield racemic **3** (*12*). Analog **3** was then coupled to the amino-derivatized cross-linked agarose support Affi-Gel 102 (Bio-Rad) through an amide bond to yield **5**; unreacted sites were blocked with acetic anhydride. The loading density was on the order of 2.1 μmol of ligand per milliliter of support (*13*). A control column was synthesized by treating the support with acetic anhydride.

A library of randomized RNA molecules was generated from a 195-nucleotide (nt) DNA template containing (i) a class three T7 promoter sequence, (ii) a 20-nt priming site for the polymerase chain reaction (PCR), (iii) a 128-nt random sequence, and (iv) another 20-nt priming site for reverse transcription and PCR amplification of the in vitro transcripts (Fig. 2). In vitro PCR amplification of the double-stranded DNA template and transcription with T7 RNA polymerase produced a 165-nt RNA. On the basis of the amount of full-length DNA template obtained from the ligation reaction of the fragments L1 and L2, the maximum complexity of the RNA pool generated is on the order of 10^{15} individual sequences. In addition to the sequence diversity, RNAs of this size should have a large number of secondary and tertiary structures.

In vitro selection was carried out with transition state analog **5**. In order to lower background absorption of RNA to the agarose, we used an acetylated agarose precolumn after the first round of selection. Selection was carried out by first heating a 2-μM solution of the RNA library in a binding buffer [200 mM NaCl, 6 mM $MgCl_2$, 5% dimethyl sulfoxide (DMSO), and 50 mM MES buffer (pH 5.75)] to 90°C and then slowly cooling it to room temperature. A 1-mg sample of the library was then passed through 2.5 ml of the affinity matrix followed by 10 column volumes of binding buffer. Bound species were then eluted with 5 mM EDTA in water and precipitated (*14*). Precipitated RNA was reverse transcribed to complementary DNA (cDNA), amplified by PCR, and transcribed to RNA with T7 polymerase; the gel-purified transcribed RNA was used directly for the next round of selection (*14*). After seven rounds of selection (*15*), the enriched RNA library was reverse transcribed, amplified by PCR, digested with the restriction enzymes Sac I and Bam HI, and ligated into the plasmid pIK-1A4 also digested with Sac I and Bam HI (*16*). Sequencing of 20 clones revealed that 16 had identical sequences (clone AA6) (Fig. 3A). The remaining four clones (AA1, AA4, AA10, and AA18) showed no obvious sequence homology to clone AA6 or to each other.

In order to determine the catalytic activity of these five clones, we performed large-scale runoff transcription reactions. The RNA product was purified by denaturing polyacrylamide gel electrophoresis and isolated from the gel by electroelution and then ethanol precipitation. When the clones (AA1, AA4, AA6, AA10, and AA18) were subsequently assayed for their ability to bind the affinity support under the elution conditions used in the selection experiments, greater than 90% of clone AA6 bound, whereas ~50% of clones AA10 and AA18 bound to the derivatized support. The remaining two clones bound acetylated agarose. Catalytic activity was then assayed in 200 mM NaCl, 6 mM $MgCl_2$, 7% DMSO, and 50 mM MES buffer (pH 5.75) at 28°C by monitoring product appearance with high-performance liquid chromatography (HPLC) (*17*). Clone AA6 was found to accelerate the isomerization of substrate **1** to product **2** above the uncata-

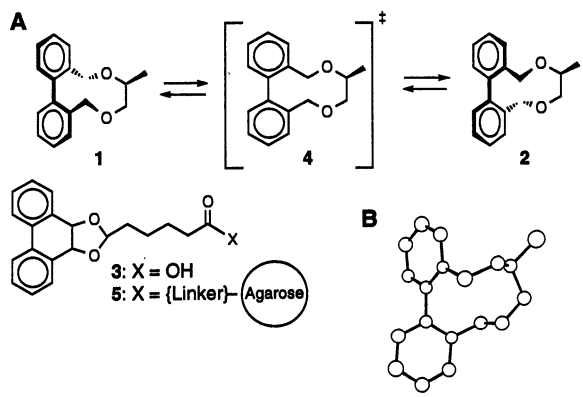

Fig. 1. (**A**) Isomerization reaction of diastereomeric biphenyl **1** to product **2** with structure of the transition state analog **3**. (**B**) X-ray crystal structure of biphenyl **2**.

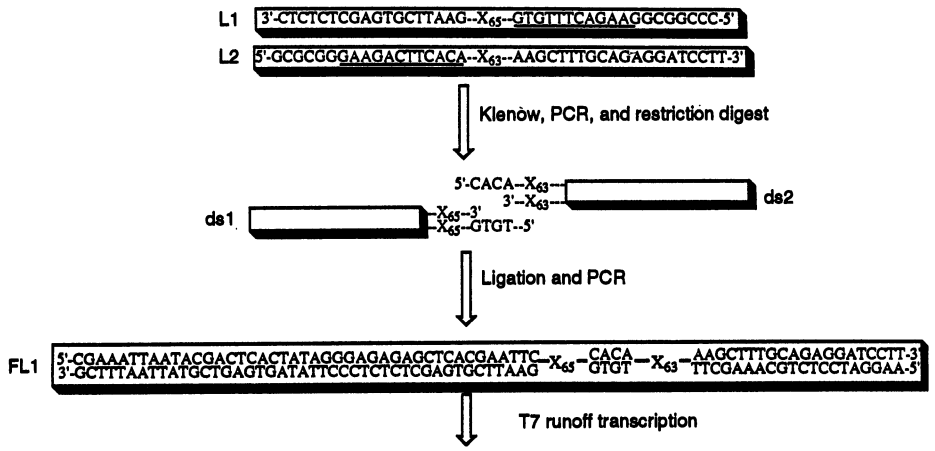

Fig. 2. Construction of RNA library consisting of a 195-nt DNA template with 128 random positions. Two synthetic 101-nt oligonucleotides, L1 and L2, were synthesized on an Applied Biosystems 391 DNA synthesizer with an equimolar mixture of the four bases in 65 positions of L1 and 63 positions of L2. Both oligonucleotides contained the underlined Bbs I sites with complementary nonpalindromic overhangs for the ensuing ligation. The deprotected synthetic oligonucleotides were purified by electrophoresis with a 6% polyacrylamide, 8 M urea gel and electroeluted with a Bio-Rad Model 422 Electro-Eluter. The oligonucleotides were converted to double-stranded form with DNA polymerase (Klenow fragment) and 20-nt primers complementary to the 3′ end. The resulting double-stranded DNAs, ds1 and ds2, were amplified by PCR in 20-ml reactions (100 reactions, 200 μl each). The amplified fragments were purified by nondenaturing polyacrylamide gel electrophoresis and eluted from the gel in 50 mM NH_4OAc (Ac, acetyl) and 10 mM $Mg(OAc)_2$ with shaking overnight at 37°C and then precipitated. The purified fragments were digested with Bbs I, purified by gel electrophoresis, and ligated with T4 DNA ligase to yield a library with an approximate complexity of 4×10^{14} molecules. Large-scale PCR was again used to generate multiple copies and to extend the 5′ arm, adding in a class three promoter site for T7 transcription. The library of full-length molecules is designated FL1.

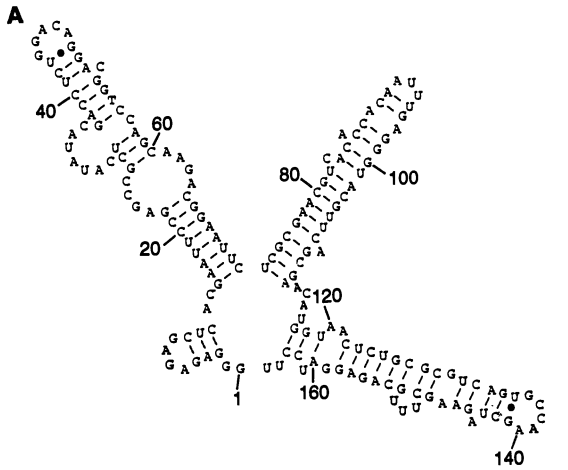

Fig. 3. (**A**) The most stable predicted secondary structure of clone AA6 (*21*). (**B**) Melting curve for clone AA6 in 220 mM NaCl, 6 mM $MgCl_2$, 5% DMSO, and 50 mM MES buffer (pH 5.75).

lyzed rate. The kinetics of this reaction were consistent with the simple mechanism

$$\text{RNA} + 1 \rightleftarrows \text{RNA}\cdot 1 \xrightarrow{k_{cat}} \text{RNA} + 2$$

in which formation of a Michaelis complex is followed by conversion to product and release. A Lineweaver-Burk plot (*18*) of the steady-state data afforded a k_{cat} of 2.8×10^{-5} min^{-1} and a K_m for substrate **1** of 542 μM; the value of k_{cat}/K_m is 5.2×10^{-2} M^{-1} min^{-1}. Multiple turnovers were observed with no loss in catalytic activity, indicating that the RNA is a true catalyst. Clones AA1, AA4, AA10, and AA18 did not catalyze the isomerization reaction (nor did a random clone isolated from the original library). In addition, treatment of clone AA6 with ribonuclease A abolished all catalytic activity. The rate of the uncatalyzed reaction (k_{uncat}) under the same conditions was determined to be 3.2×10^{-7} min^{-1}. Comparison of the first-order rate constants k_{cat} and k_{uncat} for this intramolecular reaction afforded a rate acceleration of 88-fold.

The RNA-catalyzed reaction was inhibited by the transition state analog **3**. The inhibition constant (K_i) was determined in the presence of 3, 7, and 10 μM **3** at varying substrate concentrations (*19*) (Fig. 4). Analysis of the kinetic data revealed that **3** was a competitive inhibitor with K_i = 7 μM. Because the isomerization of substrate **1** requires only rotation around a C–C sigma bond, the preferential binding of RNA to the transition state relative to ground state should correspond to the catalytic advantage in this reaction. Accordingly, $K^{\ddagger}_{RNA}/K^{\ddagger}_{uncat} = K_1/K_T = k_{RNA}/k_{uncat}$ (*20*) as defined in the scheme

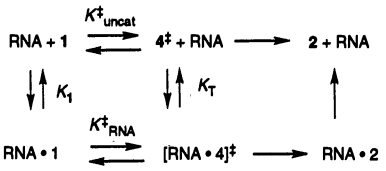

Substituting K_m(**1**) and K_i(**3**) for K_1 and K_T, respectively, affords K_1/K_T = 77, which can directly be compared with k_{cat}/k_{uncat} = 88. The similarity of these values suggests that **3** is a good analog of the planar transition state and that in this RNA-catalyzed reaction, binding energy is being utilized for catalysis. The generation of more efficient catalysts for this reaction will require the isolation of RNAs with higher preferential affinities for TS‡ analog **3**. It remains to be seen whether this is possible with a polymer consisting of only four building blocks.

The melting temperature (T_m) of clone AA6 was determined to be 70°C (Fig. 3B). The melting behavior of this clone is highly cooperative with no detectable intermediate species. Analysis of possible secondary structures for clone AA6 predicted the highly stable structure illustrated in Fig. 3A (*21*). That 16 out of 20 clones isolated had the identical sequence suggests that roughly 25 nucleotides must play important structural or catalytic roles in this RNA-catalyzed reaction (*22*, *23*).

The experiments described above suggest that even in a prebiotic world in which RNA may have acted as the primitive catalyst, the notions of transition state stabilization and binding energy in catalysis may have been realized. This approach also may prove useful in generating RNAs that exploit proximity effects, general acid-base catalysis, and covalent and electrostatic catalysis to carry out abiological reactions (*1*). Finally, this work again illustrates the productive interplay between chemistry and biology in generating biomolecules with interesting functions.

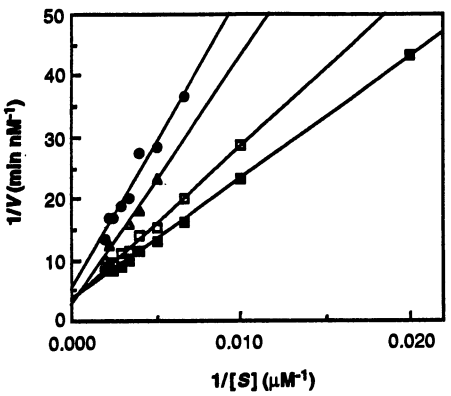

Fig. 4. Lineweaver-Burk plot for the conversion of substrate **1** to product **2** catalyzed by clone AA6. Velocities were determined by measuring initial rates by high-performance liquid chromatography monitoring at 220 nm with no inhibitor (■), 3 μM (□), 7 μM (△), or 10 μM (●), or inhibitor.

REFERENCES AND NOTES

1. S. J. Pollack, J. W. Jacobs, P. G. Schultz, *Science* **234**, 1570 (1986); A. Tramantano, K. D. Janda, R. A. Lerner, *ibid.*, p. 1566; R. A. Lerner, S. J. Benkovic, P. G. Schultz, *ibid.* **252**, 659 (1991); P. G. Schultz, *Angew. Chem. Int. Ed. Engl.* **28**, 1283 (1989).
2. J. K. Scott and G. P. Smith, *Science* **249**, 386 (1990); J. J. Devlin, L. C. Panganiban, P. E. Devlin, *ibid.*, p. 404; S. E. Cwirla, E. A. Peters, R. W. Barrett, W. J. Dower, *Proc. Natl. Acad. Sci. U.S.A.* **87**, 6378 (1990); C. F. Barbas, A. Kang, R. A. Lerner, S. J. Benkovic, *ibid.* **88**, 7978 (1991); C. Tuerk and L. Gold, *Science* **249**, 505 (1990); A. D. Ellington and J. W. Szostak, *Nature* **346**, 818 (1990); M. C. Needles *et al.*, *Proc. Natl. Acad. Sci. U.S.A.* **90**, 10700 (1993); S. P. A. Fodor *et al.*, *Science* **251**, 767 (1991).
3. D. P. Bartel and J. W. Szostak, *Science* **261**, 1411 (1993); R. Green and J. W. Szostak, *ibid.* **258**, 1910 (1992); A. A. Beaudry and G. F. Joyce, *ibid.* **257**, 635 (1992); N. Lehman and G. F. Joyce, *Nature* **361**, 182 (1993).
4. A. J. Zaug and T. R. Cech, *Science* **231**, 470 (1986); C. Guerrier-Takada, K. Gardiner, T. Marsh, N. Pace, S. Altman, *Cell* **35**, 849 (1983); O. C. Uhlenbeck, *Nature* **328**, 596 (1987).
5. J. A. Piccirilli, T. S. McConnell, A. J. Zaug, H. F. Noller, T. R. Cech, *Science* **256**, 1420 (1992); H. F. Noller, V. Hoffarth, L. Zimniak, *ibid.*, p. 1416.
6. K. Mislow, S. Hyden, H. Schaefer, *J. Am. Chem. Soc.* **84**, 1449 (1962).
7. J. B. S. Haldane, *Enzymes* (Longmans Green, London, 1930), p. 182; L. Pauling, *Chem. Eng. News* **24**, 1375 (1946).
8. J. Rebek Jr., T. Costello, R. V. Wattley, *Tetrahedron Lett.* **21**, 2379 (1980).
9. K. Mislow, M. A. W. Glass, H. B. Hopps, E. Simon, G. H. Wahl Jr., *J. Am. Chem. Soc.* **86**, 1710 (1964).
10. D. H. Hall, M. S. Lesdie, E. E. Turner, *J. Chem. Soc.* **1950**, 711 (1950).
11. Diastereomer characterization: *RS* and *SS* diastereomers were analyzed by thin-layer chromotography, nuclear magnetic resonance, mass spectrometry, elemental analysis, and melting points: fractional retention (R_f) values (a fraction of movement with respect to solvent front) (10:1, hexanes: ethyl acetate) *RS*, 0.18; *SS*, 0.23. ^1H NMR [250 MHz, $CDCl_3$, data are tabulated in the following order: multiplicity (s, singlet; d, doublet; t, triplet; q, quartet; and m, multiplet), coupling constants are in Hz] δ *RS*, 0.94 (3H, d, *J* = 6.5), 3.26 (1H, ddq, *J* = 2.4, 8.9, 6.5), 3.38 (1H, dd, *J* = 2.4, 12.2), 3.62 (1H, dd, *J* = 12.2, 8.9), 4.22 (1H, d, *J* = 11.9), 4.28 (1H, d, *J* = 12.8), 4.64 (1H, d, *J* = 11.8), 4.91 (1H, d, *J* = 12.7), 7.14 (2H, m), 7.33 (6H, m); δ *SS*, 1.10 (3H, d, *J* = 6.5), 3.23 (1H, dd, *J* = 12.9, 7.0), 3.56 (1H, ddq, *J* = 2.2, 7.0, 6.5), 3.70 (1H, dd, *J* = 2.2, 12.9), 4.44 (1H, d, *J* = 10.1), 4.52 (1H, d, *J* = 11.1), 4.54 (1H, d, *J* = 10.1), 4.80 (1H, d, *J* = 11.1), 7.12 (2H, d, *J* = 9.4), 7.36 (4H, m), 7.50 (2H, m); mass spectroscopy (fast atom bombardment) *m/e* 255.2 (MH^+) for both diastereomers; elemental analysis for $C_{17}O_2H_{18}$: C, 80.28; H, 7.13 calculated. (*RS*) C, 80.16; H, 7.28 (found); (*SS*) C, 80.02; H, 7.25

(found); melting point (*RS*) = 101° to 102°C, for (*SS*) = 112° to 114°C.
12. Phenanthrene was treated with an equimolar amount of osmium tetroxide and two equivalents of pyridine in benzene to yield the osmate ester after 7 days of stirring at 25°C. The ester was hydrolyzed with a solution of mannitol and potassium hydroxide in methylene chloride/water [R. Criegee, B. Marchand, H. Wannowius, *Ann. Chem.* **550**, 99 (1942)], and the resulting *cis*-diol was isolated by silica-gel chromatography (1:1, hexanes:ethyl acetate) after removing excess pyridine by coevaporation with *n*-heptane. Adipic acid monomethyl ester was converted to the acid chloride by treatment with an equimolar amount of oxalyl chloride in methylene chloride with a catalytic amount of dimethylformamide. The corresponding aldehyde was obtained by hydrogenation in the presence of one equivalent of 2,6-lutidine with 10% palladium on carbon in tetrahydrofuran and purified by silica-gel chromatography (3:1, hexanes:ethyl acetate). The aldehyde was combined with one equivalent of the *cis*-diol and a catalytic amount of *p*-toluenesulfonic acid monohydrate in tetrahydrofuran and stirred overnight at 25°C in the dark. The resulting acetal was purified by silica-gel chromatography (1:1, hexanes:ethyl acetate) and hydrolyzed with lithium hydroxide to yield the lithium salt of acid **3**. The ligand was dissolved in 0.1 M citric acid and extracted into chloroform to generate the free acid before coupling to the column matrix.
13. Analog **3** was coupled to both Affi-Gel 102 (Bio-Rad) and EAH Sepharose 4B (Pharmacia). The agarose matrices were slowly equilibrated in acetone, and then, for each milliliter of solvated matrix, 2.5 μmol of **3**, and equimolar amounts of benzotriazolyl-*N*-oxy-tris(dimethylamino)-phosphonium hexafluorophosphate (BOP), *N*-hydroxybenzotriazole (HOBT), and diisopropylethylamine were added. The mixture was stirred for 7 hours at 20°C with a Techne MCS-104L biological stirrer, after which time 300 μmol per milliliter of matrix of both triethylamine and acetic anhydride were added to block unreacted amines. The beads were washed five times with five bed volumes of acetone and stored at −20°C. Control columns were blocked with acetic anhydride and triethylamine in a similar fashion. In order to determine the extent of derivatization of the support, we incubated monoclonal antibodies specific for analog **3** with the affinity supports in phosphate-buffered saline (PBS) containing 10% calf serum for 1 min. The beads then were washed four times with five volumes of PBS and analyzed with alkaline phosphatase–conjugated goat antibodies to mouse immunoglobulin.
14. The cDNAs were prepared from eluted RNAs by reverse transcription. The reactions were carried out in 20 μl of buffer [10 mM tris-HCl (pH 8.9), 50 mM KCl, 2 mM $MgCl_2$, 0.01% gelatin, and 0.1% Triton X-100 containing 1.25 mM of each deoxynucleotide triphosphate, 5 μM of each 5′ and 3′ extension primer, and 10 U of avian reverse transcriptase] for 20 min at 50°C. The PCR reactions were carried out in the identical tube after the addition of 180 μl of the above reaction buffer with the addition of 5 U of Taq polymerase. Reactions were cycled through 1 min at 94°C and 1 min at 54°C until ~10 μg of double-stranded DNA was obtained. The PCR reaction mixture (50 μl) was added directly to 250 μl of a transcription cocktail containing 40 mM tris-HCl (pH 7.8), 5 mM dithiothreitol, 20 mM $MgCl_2$, 5 mM of each ribonucleoside triphosphate, and 3750 U of T7 RNA polymerase and then incubated for 2 hours at 41°C to yield ~1 mg/ml of full-length transcript.
15. The seventh round of selection was carried out with the TS analog **3** immobilized on an EAH Sepharose 4B support (which contains an extended tether and non–cross-linked agarose). After this final round, less than 1% of the enriched library bound the acetylated Sepharose control column, whereas >85% bound the affinity support.
16. The plasmid pIK-1A4 is a pUC19 derivative containing a Sac I–Bam H1 cloning site after the class three T7 RNA polymerase promoter.
17. Reactions were followed by HPLC with a Microsorb C18 reversed-phase column (Rainin Instruments) and a mobile phase of 70% acetonitrile in water over 11 min by monitoring ultraviolet absorbance at 220 nm. Product **2** was identified by co-injection with authentic material.
18. I. H. Segel, *Enzyme Kinetics* (Wiley, New York, 1975), p. 46.
19. Inhibition reactions were carried out at 50, 100, 150, 200, 250, 300, 350, 400, 450, and 500 μM substrate **1** and 10 μM RNA in assay buffer at 28°C.
20. W. P. Jencks, *Adv. Enzymol. Relat. Areas Mol. Biol.* **43**, 219 (1975).
21. M. Zuker, *Science* **244**, 48 (1989); J. A. Jaeger, D. H. Turner, M. Zuker, *Proc. Natl. Acad. Sci. U.S.A.* **86**, 7706 (1989).
22. There are a maximum of 10^{15} or roughly 4^{25} sequences in the RNA library. If 25 bases are strictly required for catalysis, one might expect to find a single unique sequence in the library.
23. Selection of the RNA library against TS analog **3** at pH 7.5 under otherwise identical conditions afforded 2 out of 12 clones with the identical sequence to clone AA6.
24. We are grateful for financial support for this work from the Office of Naval Research (grant #N00014-91-J-1130) and from the Director, Office of Health Effects Research, of the U.S. Department of Energy under contract no. DE-AC03-76SF00098. J.R.P. was supported by NIH Biotechnology Training Grant GM08352A. We thank J. Szostak and J. Lorsch for helpful discussions.

8 March 1994; accepted 4 May 1994

A Low-Barrier Hydrogen Bond in the Catalytic Triad of Serine Proteases

Perry A. Frey, Sean A. Whitt, John B. Tobin

Spectroscopic properties of chymotrypsin and model compounds indicate that a low-barrier hydrogen bond participates in the mechanism of serine protease action. A low-barrier hydrogen bond between Nδ1 of His^{57} and the β-carboxyl group of Asp^{102} in chymotrypsin can facilitate the formation of the tetrahedral adduct, and the nuclear magnetic resonance properties of this proton indicate that it is a low-barrier hydrogen bond. These conclusions are supported by the chemical shift of this proton, the deuterium isotope effect on the chemical shift, and the properties of hydrogen-bonded model compounds in organic solvents, including the hydrogen bond in *cis*-urocanic acid, in which the imidazole ring is internally hydrogen-bonded to the carboxyl group.

The mechanism by which the catalytic triad in serine proteases catalyzes the hydrolysis of peptide bonds has long been debated. In chymotrypsin, the triad consists of Ser^{195}, His^{57}, and Asp^{102}. Spectroscopic evidence indicates that a strong hydrogen bond (a low-barrier hydrogen bond or LBHB) links His^{57} and Asp^{102} in the protonated state of the catalytic triad. The formation of an LBHB between His^{57} and Asp^{102} in the course of catalysis should increase the reactivity of His^{57} as a general base. We postulate a new mechanism in which the formation of this LBHB facilitates nucleophilic attack by the β-OH group of Ser^{195} on the acyl carbonyl group of substrates.

Hydrogen bonds have been classified in three types (*1*): (i) weak or conventional (2.4 to 12 kcal mol^{-1}); (ii) strong or low-barrier (12 to 24 kcal mol^{-1}); and (iii) very strong or single-well (>24 kcal mol^{-1}). The potential energy wells in Fig. 1 represent these types for a system where a proton between two heteroatoms is exchanged $\mathbf{A-H\cdots B} \leftrightarrows \mathbf{A\cdots H-B}$. An example of very strong hydrogen bonding is provided by hydrogen difluoride ($[FHF]^-$) (*1*, *2*), in which the distance between fluorine atoms is 2.26 Å and the hydrogen bond energy is 37 kcal mol^{-1}. Low-barrier and single-well hydrogen bonds may be represented as $\mathbf{A|||H|||B}$.

Strong hydrogen bonds can form when the distance between the heteroatoms ($R_{A\cdots B}$) is less than the sum of the van der Waals radii (<2.55 Å for O–H–O and <2.65 Å for O–H–N) and the change in the negative logarithm of the acid constant (ΔpK_a) between the heteroatoms is near 0 (*1*, *3*, *4*). Medium effects are important because values for pK_a are dependent on solvent; that is, variant pK_a's of two acidic groups in water may become similar in an organic solvent or in a crystalline state.

The most definitive physical characterization of an LBHB is the measurement of $R_{A\cdots B}$ by x-ray crystallography or neutron diffraction. In most cases, however, the structures of proteins are not known with enough accuracy to distinguish values of $R_{A\cdots B}$ between 2.5 Å and 2.7 Å. Of the four other physicochemical parameters for characterizing LBHBs (*1*), the most unambiguous is the nuclear magnetic resonance (NMR) chemical shift δ_H for a participating proton, which ranges from 16 to 20 parts per million (ppm). Three parameters depend on the effects of deuterium on the hydrogen bond. The isotope effect on infrared stretching frequencies is the ratio ν_{AH}/ν_{AD}, the isotope effect on the NMR chem-

Institute for Enzyme Research, Graduate School, and Department of Biochemistry, College of Agricultural and Life Sciences, University of Wisconsin at Madison, Madison, WI 53705, USA.